AGU PUBLICATIONS

JGR

Journal of Geophysical Research: Space Physics

RESEARCH ARTICLE

10.1002/2015JA022111

Key Points:

- BTEC/GPS-TEC had obvious diurnal variations
- BTEC/ITEC agreed with BTEC/GPS-TEC for positive phase but not for nighttime or negative phase
- Plasmaspheric contribution and plasma temperatures are important for topside ionospheric response

Correspondence to:
J. Lei,
leijh@ustc.edu.cn

Citation:
Zhu, Q., J. Lei, X. Luan, and X. Dou (2016), Contribution of the topside and bottomside ionosphere to the total electron content during two strong geomagnetic storms, *J. Geophys. Res. Space Physics*, *121*, 2475–2488, doi:10.1002/2015JA022111.

Received 2 NOV 2015
Accepted 10 FEB 2016
Accepted article online 12 FEB 2016
Published online 4 MAR 2016

Contribution of the topside and bottomside ionosphere to the total electron content during two strong geomagnetic storms

Qingyu Zhu[1], Jiuhou Lei[1,2,3], Xiaoli Luan[1], and Xiankang Dou[1]

[1]CAS Key Laboratory of Geospace Environment, School of Earth and Space Sciences, University of Science and Technology of China, Hefei, China, [2]Mengcheng National Geophysical Observatory, University of Science and Technology of China, Hefei, China, [3]Collaborative Innovation Center of Astronautical Science and Technology, Harbin, China

Abstract In this study, the ionospheric observations from ionosondes, GPS receivers, and incoherent scatter radars (ISR) at low and middle latitudes were used to investigate the contribution of the bottomside and topside ionosphere to the total electron content (TEC) during the September 2005 and December 2006 geomagnetic storms. It was found that the contribution of the bottomside TEC below F_2 peak (BTEC) to the ionosonde ionospheric TEC (ionosonde ITEC), namely, BTEC/ITEC was almost constant during both quiet and storm times, while the ratio of BTEC to GPS TEC (i.e., BTEC/GPS-TEC) underwent obvious diurnal variations at all stations. The BTEC/GPS-TEC during the positive phase was similar to that during quiet time, regardless of the formation mechanisms of the observed positive phases. Moreover, our analysis revealed that the ISR calculated BTEC/ITEC during positive ionospheric phases was comparable to that during quiet time. This suggests that the positive phases in these two events mainly occurred around the F_2 peak height. There were large differences between the calculated BTEC/ITEC from the ISR observations and BTEC/GPS-TEC during the negative phase or at night when the plasmasphere possibly contributed significantly to the TEC in the relative sense. Although the absolute changes of the topside TEC were larger than the bottomside TEC at low and middle latitudes associated with the larger topside effective ionospheric thickness, unlike the October 2003 superstorms, the relative changes of the topside TEC to the quiet time reference in these two strong storms were not greater than the changes of the bottomside TEC and peak density N_mF_2.

1. Introduction

Ionospheric electron densities can increase or decrease in response to geomagnetic storm associated with the significantly enhanced injection of energy originating from solar wind [e.g., *Prölss*, 1995; *Buonsanto*, 1999]. Ionospheric storm effects have been extensively studied on the basis of the observations of F_2 peak density (N_mF_2) and total electron content (TEC) [e.g., *Prölss*, 1995; *Mendillo*, 2006]. However, the topside ionospheric response to the storm is yet well explored, given that the topside ionospheric observations are relatively sparse [e.g., *Lei et al.*, 2014, 2015; *Gulyaeva and Stanislawska*, 2013, and references therein]. Although incoherent scatter radar (ISR) is a powerful tool for the direct measurement of ionosperic parameters from ionospheric E region to the topside ionosphere, the ISR sites and operational time are limited.

There were several approaches to study the storm time topside ionospheric response. *Huang and Reinisch* [2001] developed a method to derive the topside density based on the observation of ionosonde bottomside electron density. This method has a big assumption that the topside electron density follows the α-Chapman function with the same scale height as the bottomside electron density profile. *Belehaki and Tsagouri* [2002] utilized Huang and Reinisch method to investigate the contribution of bottomside TEC to the full TEC in the ionosphere during several weak and moderate storms over Athens. Although the applicability of the extrapolated topside ionospheric profile was examined in many studies under the quiet time condition [e.g., *Reinisch et al.*, 2007; *Stankov et al.*, 2003; *Verhulst and Stankov*, 2015], whether the ionosonde topside profile is suitable for the storm study is not addressed.

Another method, which was used recently, is to combine ionospheric observations from ionosonde and ground-based GPS receivers [e.g., *Zhao et al.*, 2012; *Lei et al.*, 2015]. The topside TEC above the F_2 peak height can be obtained from the difference between GPS TEC and bottomside electron content derived from ionosonde measurements. In addition, the observations of up-looking TEC from low Earth orbit (LEO) satellites can also provide important information of the topside ionosphere [e.g., *Mannucci et al.*, 2005;

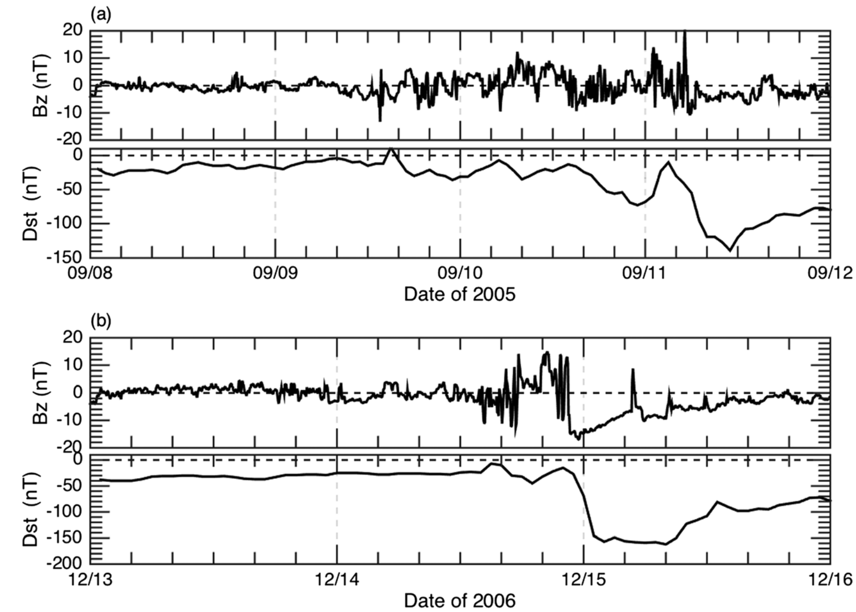

Figure 1. Variations of IMF Bz component and *Dst* index during (a) 8–11 September 2005 and (b) 13–15 December 2006.

Astafyeva, 2009; *Lei et al.*, 2014, 2015; *Astafyeva et al.*, 2015]. However, the up-looking LEO TEC represents TEC values above the satellite orbital altitudes, so that sometimes the observed up-looking TEC change can be possibly associated with the movement of the F_2 peak height if the up-looking TEC changes are not profound.

Recently, *Lei et al.* [2015] combined ionospheric observations from the ground-based GPS receiver network, LEO satellites, and ionosondes to examine topside and bottomside ionospheric response to the October 2003 superstorms. They suggested that the absolute changes in the topside TEC during storm time should be larger than in the bottomside TEC, which is due to a larger topside ionospheric thickness. However, they further addressed that the topside ionospheric enhancements were much stronger than those seen in N_mF_2 and bottomside TEC in terms of relative changes with respect to the quiet time reference. Note that *Lei et al.* [2015] devoted to the topside ionospheric response to the 2003 October superstorms when the solar wind drivers were extremely strong. Whether the topside and bottomside ionosphere also respond differently to strong geomagnetic storm rather than superstorm becomes an objective of this study. We will examine the differences and similarities of the topside and bottomside ionospheric response to two strong geomagnetic storms.

In this study, we focused on the topside and bottomside ionospheric response to the September 2005 and December 2006 strong storms in the American sector by using observations from ionosondes, ground-based GPS receivers, and ISRs. Previous studies revealed that the changes of equatorward neutral winds and electric fields were the major mechanisms for the positive phases of September 2005 storm [*Lu et al.*, 2008] and December 2006 storm [*Lei et al.*, 2008], respectively. Thus, it allows us to study the evolvement of bottomside and topside ionosphere during the storm time associated with different mechanisms. Moreover, the ionospheric data showed obvious positive and negative ionospheric storm phases during both storms. Therefore, we can examine how the topside and bottomside ionospheric response depends on ionospheric storm phase.

2. Geophysical Conditions of September 2005 and December 2006 Storms

The variations of interplanetary magnetic field (IMF) Bz component and *Dst* index during 8–11 September 2005 are shown in Figure 1a. The changes of Bz were relatively small on 8 September, and Bz started to fluctuate at 14:00 UT on 9 September. These Bz oscillations persisted till 6:00 UT on 11 September. After that, Bz kept southward during the rest time of 11 September. The ring current *Dst* had two strong minima on 10 and 11 September, which were about −80 nT and −140 nT, respectively.

Figure 1b shows the evolutions of IMF Bz component and *Dst* index on 13–15 December 2006. Obviously, on 13 December, Bz and *Dst* were stable so that geomagnetic activity condition was quiet. At 14:00 UT on 14

December, Bz underwent notable fluctuations and *Dst* had an obvious increase, which was associated with the SSC of the storm. From 22:30 UT on 14 December, Bz started to stay southward and kept stable southward direction almost for the whole day of 15 December. Consequently, *Dst* reached the minimum of −170 nT at 6:00 UT on 15 December and then gradually recovered.

These two storms happened in the decline phase of solar cycle 23. The mean solar flux proxy $F_{10.7}$ was about 106 and 90 for September 2005 and December 2006 storms, respectively. According to the definition of geomagnetic storm category [*Gonzalez et al.*, 1994], these were strong storms. We compare the topside and bottomside response to these two strong storms with that seen in the October 2003 superstorms in which the minimum *Dst* reached about −400 nT.

3. Ionospheric Data Set

The ionospheric observations from ground-based GPS receivers, ionosondes, and ISRs were used in this study. The derivation of ground-based TEC has been described in previous studies [e.g. *Mannucci et al.*, 1998; *Rideout and Coster*, 2006]. First, the relative line-of-sight TEC was obtained by leveling the phase delay of pseudorange signals. After removing GPS satellites biases and receiver bias, the absolute line-of-sight TEC was converted to the vertical TEC by using the mapping function. The ground-based GPS data used in this study were obtained from the Massachusetts Institute of Technology (MIT) Haystack Observatory Madrigal database (http://madrigal.haystack.mit.edu/).

We used simultaneous GPS TEC and ionosonde data from four stations in the American sector: Jicamarca (12°S, 76.8°W), Ramey (Arecibo) (18.5°N, 67.1°W), Eglin (30.5°N, 86.5°W), and Millstone Hill (42.6°N, 71.5°W) during both September 2005 and December 2006 storms. The temporal resolutions for the used ionograms were either 15 or 5 min. The ionospheric peak height (h_mF_2) and peak density (N_mF_2) along with the integrated electron content below the F_2 peak, namely, BTEC, were used to further provide information about ionospheric densities in the F_2 layer.

However, the ionosonde cannot provide direct observations of electron density above F_2 peak height. As mentioned previously, *Huang and Reinisch* [2001] introduced a method to estimate the topside electron density from the α-Chapman function extrapolation, i.e., the topside electron density N_T can be given by

$$N_T = N_mF_2 \cdot \exp\left[\frac{1}{2}\left(1 - z - e^{-z}\right)\right]. \quad (1)$$

In equation (1), $z = \frac{h - h_mF_2}{H_T}$, where H_T is the Chapman scale height at the topside ionosphere and is assumed to be equal to the scale height around the F_2 peak. Then the estimated ionosonde topside TEC (TTEC) is given as

$$\mathrm{TTEC} = \int_{h_mF_2}^{1000} N_T \, \mathrm{d}h. \quad (2)$$

Thus, the ionosonde ionospheric TEC (ionosonde ITEC) is the sum of BTEC and TTEC. Although the ionosonde ITEC was used in previous studies [e.g., *Belehaki and Tsagouri*, 2002], its applicability during storm time should downgrade significantly. In this study, we compared the ionosonde TEC and GPS TEC at low and middle latitudes to verify whether the calculated ionosonde TEC is consistent with GPS TEC. Note that only Chapman function is considered here for the topside profile extrapolation, since it has been embedded in the SAO-explorer software [*Huang and Reinisch*, 2001].

The ISR can provide electron density measurement in the whole *F* region. Ionospheric observations at both Arecibo and Millstone Hill ISRs during the September 2005 storm and at Millstone Hill during the December 2006 storm period were used in this study. The time resolution for the Millstone Hill ISR data was about 16 min during September 2005 storm and ~10 min during December 2006 storm, while the temporal resolution for the Arecibo ISR data was 1–2 min during September 2005 storm. The ISR N_mF_2 and h_mF_2 were derived from the observed profiles using a least squares fitting, and then BTEC is calculated from electron densities below h_mF_2 and ITEC is the integration of electron densities between 100 and 700 km. Note that at nighttime the Arecibo ISR observations had the data gap region at low altitudes, where the signal to noise ratio is very low when the electron density is lower than 10^9 m^{-3}. If we assume the height of the gap region is 100 km, and the maximum TEC value for this gap is $10^9 \times 10^5$ m^{-2} = 0.01 total electron content unit, 1 TECU = 10^{16} el m^{-2}. Thus, the data gap will not affect our calculations. Additionally, the difference

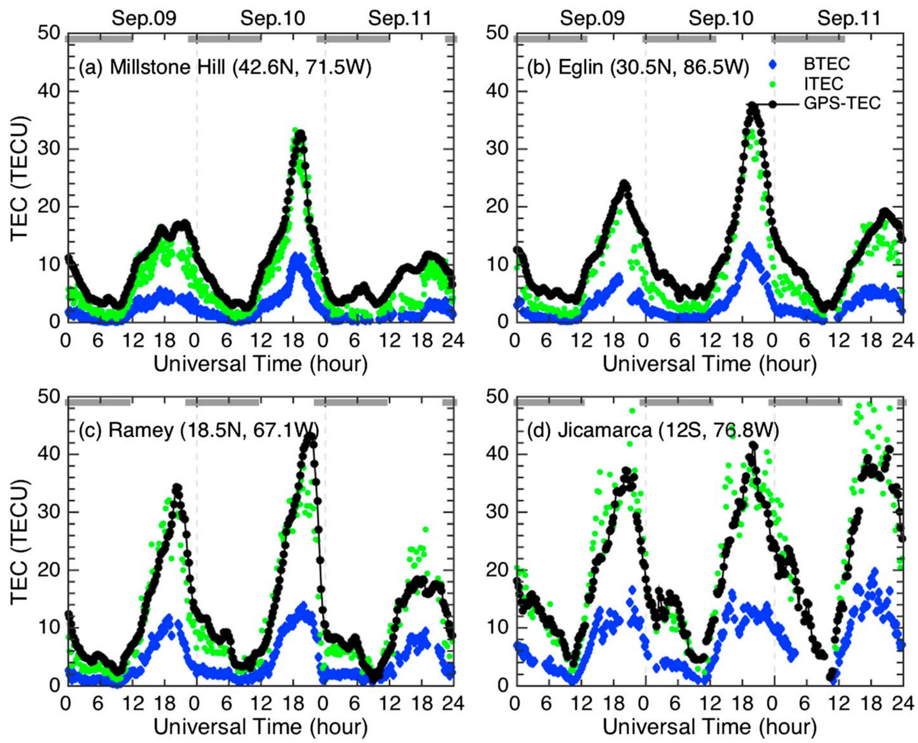

Figure 2. Comparison between ionosonde BTEC (blue) and ITEC (green) and GPS TEC (black) at four stations during 9–11 September 2005. The grey bars in this figure and the following figures represent nighttime.

between GPS TEC and ionosonde bottomside TEC, standing for the TEC above the F_2 peak, was designated the topside TEC [see *Lei et al.*, 2015], since the ISRs cannot give the plasmaspheric contribution to the TEC.

4. Observations and Results

In this section, we present the observational results from ionosondes, ground-based GPS receivers, and ISRs during the periods of the September 2005 and December 2006 storms.

4.1. September 2005 Event

Figure 2 shows the comparison between GPS TEC (black) and ionosonde derived ITEC (green) at low and middle latitude stations in the American sector during 9–11 September 2005. The observations on 9 September instead of 8 September were used as the quiet time references due to data gaps in the ionosonde observations on 8 September. The ionosonde derived ITEC was generally consistent with GPS TEC. However, at nighttime the ionosonde ITEC was lower than GPS TEC at Millstone Hill, Eglin, and Ramey. Compared with TEC on 9 September, both ITEC and GPS TEC had a predominant enhancement in daytime of 10 September and a decrease on 11 September with the exception at Jicamarca where GPS TEC did not show obvious changes. Therefore, positive and negative storm effects occurred at low and middle latitudes on 10 and 11 September, respectively, in terms of the TEC changes with respect to TEC on 9 September. The bottomside TEC (BTEC) obtained from ionosonde data was also shown in this figure. It is clear that the variations of BTEC were in phase of those of ITEC and GPS TEC, although the changes in BTEC were much smaller than in ITEC and GPS TEC.

To assess the contribution of BTEC to the full ionospheirc TEC, we calculated the ratios, BTEC/ITEC and BTEC/GPS-TEC. The reasons to focus on BTEC/ITEC and BTEC/GPS-TEC are given as follows. If we consider BTEC = $N_mF_2 * \tau_B$ and TTEC = $N_mF_2 * \tau_T$, then we have $\text{BTEC/ITEC} = 1/\left(1 + \frac{\tau_T}{\tau_B}\right)$, where τ_B, τ_T are the bottomside and topside effective thickness, respectively. Therefore, the evolutions of BTEC/ITEC and BTEC/GPS-TEC from quiet to storm periods would provide important information about the variations of the ionospheric profile shape or effective ionospheric thickness.

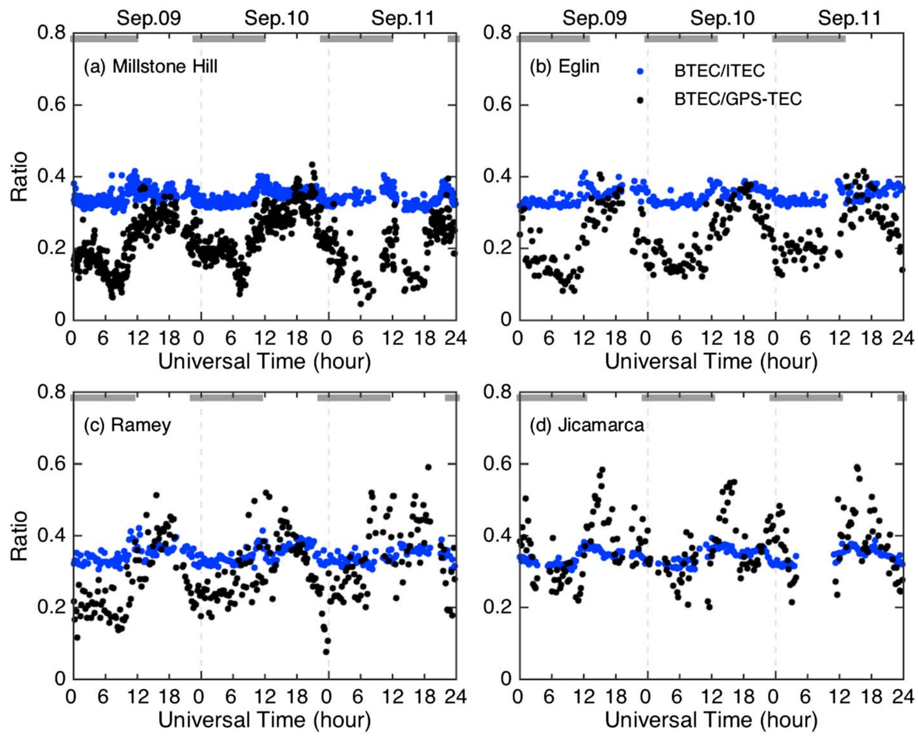

Figure 3. Comparison between BTEC/ITEC (blue) and BTEC/GPS-TEC (black) during 9–11 September 2005. Here BTEC and ITEC are obtained from ionosonde data.

As shown in Figure 3, BTEC/GPS-TEC underwent obvious diurnal variations with a larger ratio in daytime. However, BTEC/ITEC had less diurnal variations and it almost kept a constant value (~0.3–0.4) at a given station, regardless of quiet or storm times. Also, it is clear that the difference between BTEC/ITEC and BTEC/GPS-TEC was significant at night except at the magnetic equatorial station Jicamarca where larger difference between them was seen in daytime. For the ratio BTEC/GPS-TEC, it did not have obvious changes on 10 and 11 September as compared with those on 9 September. However, at Millstone Hill, the BTEC/GPS-TEC became lower in the daytime of 11 September when the negative phase was strong.

In Figure 3, the ionosonde BTEC/ITEC was almost a constant value. Given that the ionosonde topside profile is extrapolated from the bottomside ionosphere, this constant ratio is expected, if we consider that $\int_{-4}^{0}\exp\left[\frac{1}{2}\left(1-z-e^{-z}\right)\right]dz/\int_{-4}^{\infty}\exp\left[\frac{1}{2}\left(1-z-e^{-z}\right)\right]dz \approx 0.32$, although in this calculation we extrapolated Chapman function in the bottom side (from h_mF_2 down to the altitude of four scale heights below). Physically, BTEC/ITEC should be always larger than BTEC/GPS-TEC if ITEC is correctly calculated and GPS-TEC is precisely measured. Compared with BTEC/GPS-TEC, larger BTEC/ITEC occurred sometimes, which might be associated with the uncorrected approximation in the ionosonde topside profiles. Nevertheless, it should be noted that the difference between BTEC/ITEC and BTEC/GPS-TEC might be also related to the contribution of TEC in plasmasphere (PTEC) [e.g., *Belehaki and Tsagouri*, 2002]. The ISR observation can provide more information about BTEC/ITEC and then give some insight of plasmaspheric contribution to the full TEC. Next, we show the ISR observations at Arecibo and Millstone Hill during the September 2005 storm.

Figure 4 shows the ISR observations at Arecibo during the September 2005 storm. As shown in Figures 4a–4c, significant positive phase took place on September 10 along with the increases of h_mF_2 and N_mF_2 as compared with their quiet time references on 8 September. Meanwhile, the ionospheric parameters derived from ionosonde were in a remarkable agreement with those from the ISR in this event (Figures 4b and 4c), and N_mF_2 and h_mF_2 decreased on 11 September. In Figure 4d, the ISR calculated ITEC was in good agreement with GPS TEC. Similar to ionosonde BTEC, the ISR BTEC was also in phase with ISR ITEC and GPS TEC. The calculated ratios BTEC/ITEC and BTEC/GPS-TEC from ISR and GPS data are shown in Figure 4e. Although the ITEC and GPS-TEC had more obvious changes during storm time, the ISR calculated BTEC/ITEC stayed

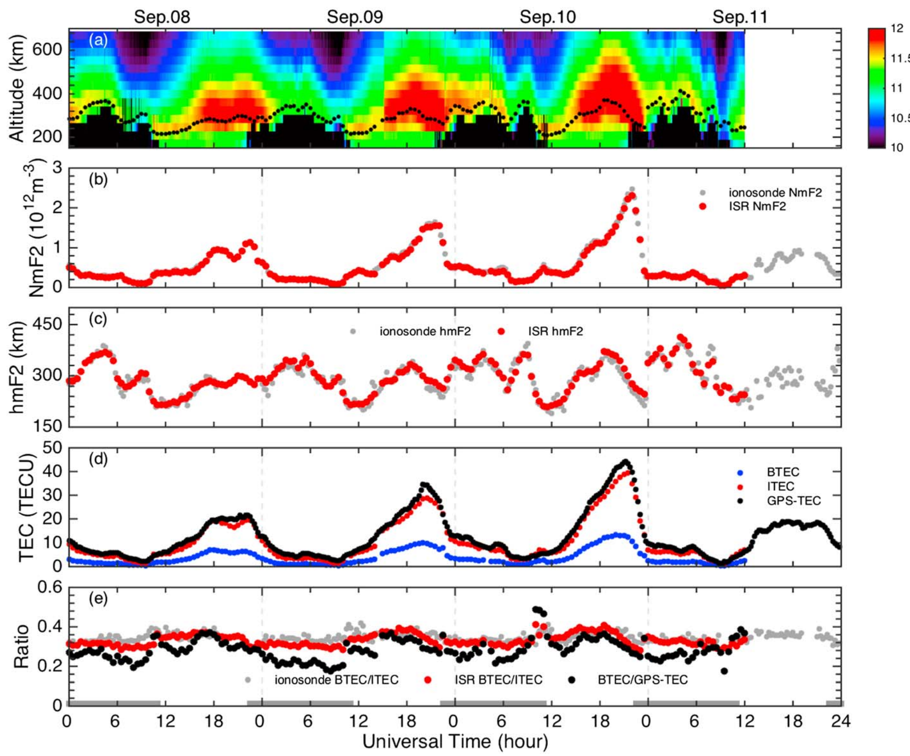

Figure 4. Ionospheric observations at Arecibo during 8–11 September 2005. From the top to bottom panel are: (a) ISR electron density contour (black dots represent h_mF_2), (b) N_mF_2 and (c) h_mF_2 obtained from ISR and ionosonde, (d) BTEC and ITEC derived by ISR and GPS TEC, and (e) BTEC/GPS-TEC (black), and ISR (red) and ionosonde (grey) calculated BTEC/ITEC.

at ~0.3–0.4 during 8–11 September, which is consistent with ionosonde results (grey line). Additionally, the ratio BTEC/GPS-TEC during the storm time was similar to the quiet time value. This suggests that at Arecibo the observed positive and negative storm effects on 10–11 September mainly occurred around the F_2 peak height, and electron densities did not change significantly at the altitudes above h_mF_2 by 2–3 scale heights. However, diurnal variation of BTEC/GPS-TEC was larger than that of BTEC/ITEC. Large differences between BTEC/ITEC and BTEC/GPS-TEC were observed at night. This indicates that electron densities above 700 km (or plasmasphere) contribute significantly to the full TEC at night when ionospheric plasma density is low.

Figure 5 shows the ISR observations at Millstone Hill during the September 2005 storm, with the same format as Figure 4. Compared with 8 September, electron densities in the F_2 layer on 9 September showed a slight increase (Figures 5a and 5b), although the peak height h_mF_2 did not show an elevation (Figure 5c). The ISR ITEC, N_mF_2, and GPS TEC (Figures 5b and 5d) showed that a consistent positive storm effect occurred on 10 September when peak height h_mF_2 was raised from ~210 km on 8 September to ~360 km on September 10 (Figure 5c). Strong depletions were observed in N_mF_2, ITEC, and GPS TEC on 11 September accompanying with large decrease of h_mF_2. In the daytime of 11 September, h_mF_2 dropped to a minimum height of ~150 km. This feature is called as "G" condition [e.g., *Buonsanto*, 1999] when the storm time neutral composition disturbance is very strong so that the whole F_2 layer is almost eaten away. Surprisingly, as shown in Figure 5e, the shape of ISR obtained BTEC/ITEC was generally consistent with that of BTEC/GPS-TEC, even at nighttime. Besides, the ISR related BTEC/ITEC agreed well with that from the ionosonde data (grey line), except for at night when the ionosonde BTEC/ITEC was high. Again, no clear changes were seen in the BTEC/ITEC and BTEC/GPS-TEC on 10 September when the strong ionospheric positive storm effect occurred. However, as shown in Figure 3a, the ionosonde BTEC/GPS-TEC decreased on 11 September when the G condition happened. In this case, the whole F_2 region was washed out and the plasmasphere had significant contribution, so that BTEC became less important in relative with the full TEC, which is similar to the nighttime situation.

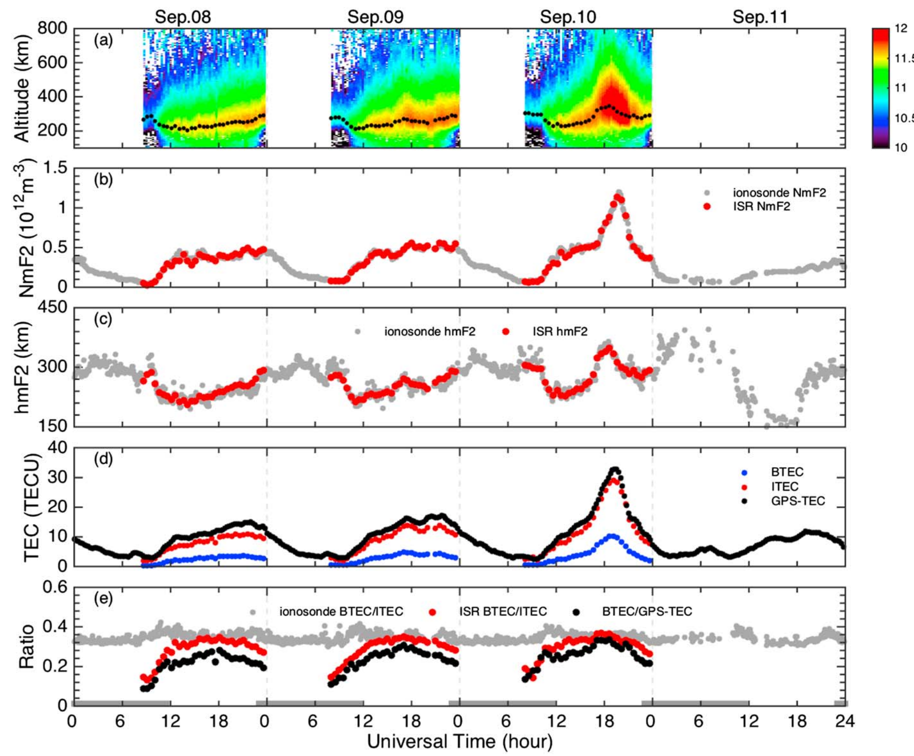

Figure 5. Ionospheric observations at Millstone Hill during 8–11 September 2005. (top to bottom) (a) ISR electron density contour (black dots represent h_mF_2), (b) N_mF_2 and (c) h_mF_2 obtained from ISR and ionosonde, (d) BTEC and ITEC derived by ISR and GPS TEC, and (e) BTEC/GPS-TEC (black), and ISR (red) and ionosonde (grey) calculated BTEC/ITEC.

4.2. December 2006 Event

Figure 6 shows evolutions of GPS TEC and ionosonde derived TEC in the American sector during 13–15 December 2006. A positive ionospheric phase was observed in GPS TEC on 14 December at Millstone Hill, Eglin, and Ramey as compared with the quiet time values on 13 December. *Lei et al*. [2008] revealed that the positive storm effects at low and middle latitudes were associated with prompt penetration electric fields (PPEF) during the storm initial phase. A negative ionospheric phase occurred on 15 December was observed at Millstone Hill, Eglin, and Ramey. Moreover, the TEC depletion was greater at Millstone Hill and Eglin than at lower latitude station Ramey. As for equatorial station Jicamarca, GPS TEC stayed at high level during 13–15 December and was higher than at other three stations. We also compared the TEC derived from ionosonde with GPS TEC. The ionosonde ITEC was generally consistent with GPS TEC at Millstone Hill, Eglin, and Ramey, except that it obviously underestimated nighttime TEC level. However, at Jicamarca, the daytime ionosonde ITEC was larger than GPS TEC (Figure 6d), which is consistent with the result in the September 2005 storm.

Figure 7 shows the comparison between BTEC/ITEC for ionosonde and BTEC/GPS-TEC during the December 2006 storm. It is obvious that the ionosonde BTEC/ITEC was about ~0.3–0.4 while BTEC/GPS-TEC had more notable diurnal variations during both quiet and storm times. Similar to the September 2005 storm, BTEC/ITEC and BTEC/GPS-TEC showed significant discrepancy at night and they were close in daytime at low and middle latitudes. Moreover, the BTEC/GPS-TEC during the positive phase on 14 December was quite similar to that during quiet time (13 December). Nevertheless, at Millstone Hill and Ramey the BTEC/GPS-TEC on 15 December, when the negative phase took place, was different with that on 13 December. Specifically, it was lower at Millstone Hill and higher at Ramey on 15 December as compared with the quiet time values. At the equatorial station Jicamarca, the BTEC/GPS-TEC was larger than BTEC/ITEC in the daytime during 13–15 December. The diurnal variations and latitudinal dependence of BTEC/GPS-TEC during the December 2006 storm were similar to those during the September 2005 storm.

The Millstone Hill ISR observations are shown in Figure 8 to provide further information about the electron density profiles during the December 2006 storm. Note that the Arecibo radar was off during this period.

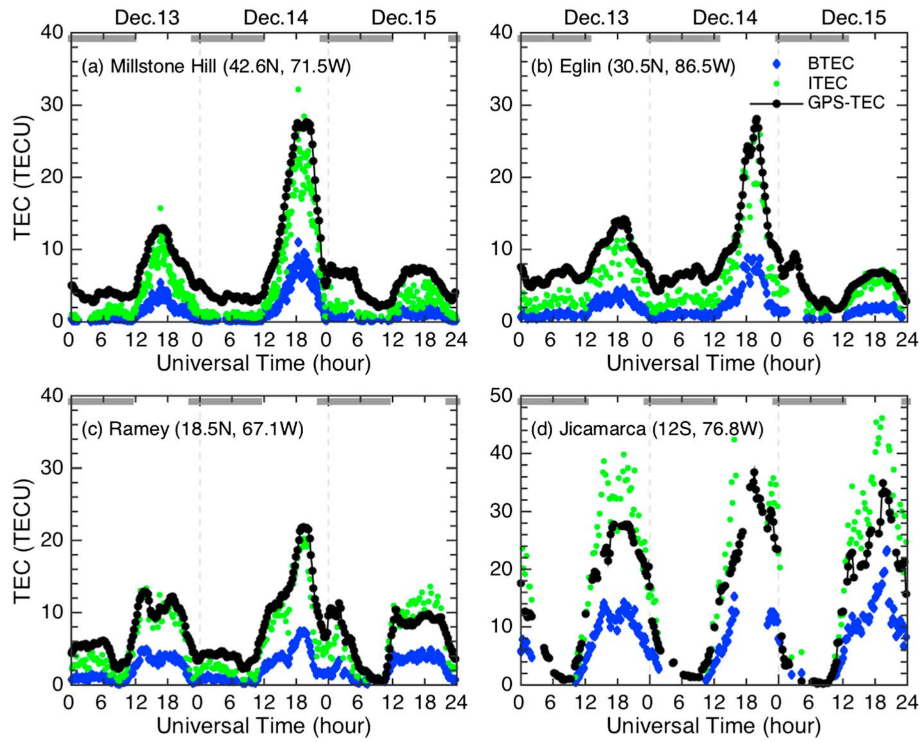

Figure 6. Comparison between ionosonde BTEC (blue) and ITEC (green) and GPS TEC (black) at four stations during 13–15 December 2006.

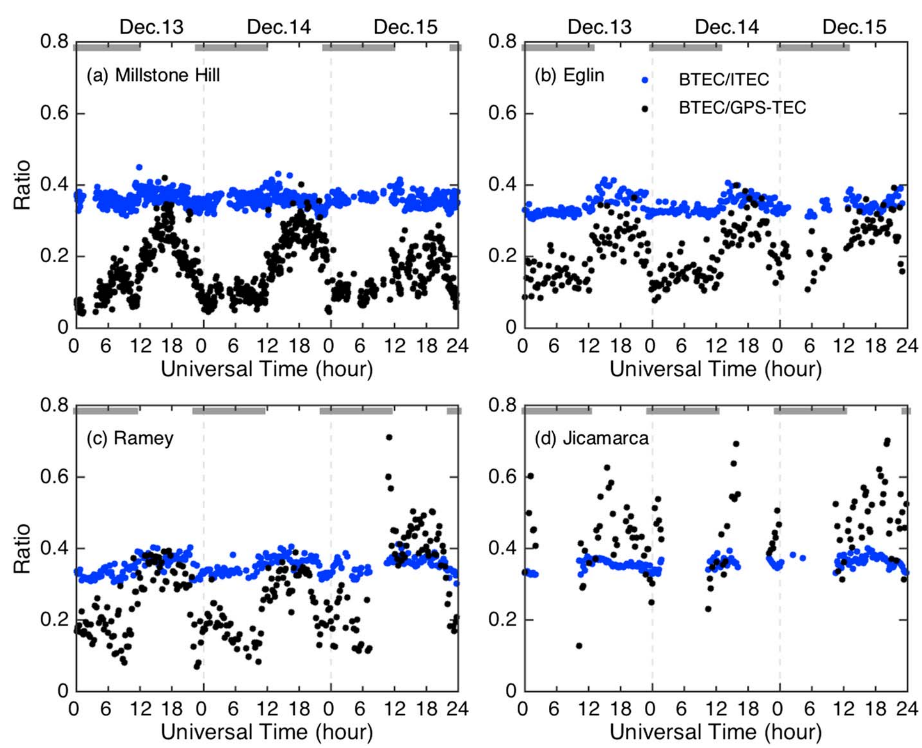

Figure 7. Comparison between BTEC/ITEC (blue) and BTEC/GPS-TEC (black) during 13–15 December 2006. Here BTEC and ITEC are obtained from ionosonde data.

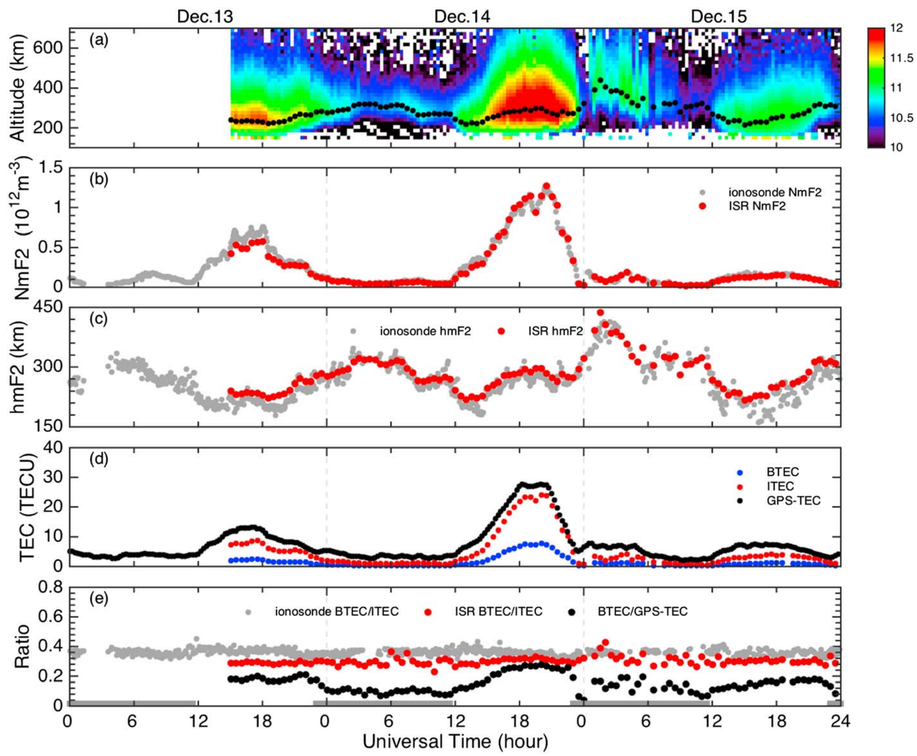

Figure 8. Ionospheric observations over Millstone Hill during 13–15 December 2006. (top to bottom) (a) ISR electron density contour (black dots represent h_mF_2), (b) N_mF_2 and (c) h_mF_2 obtained from ISR and ionosonde, (d) BTEC and ITEC derived by ISR and GPS TEC, and (e) BTEC/GPS-TEC (black), and ISR (red) and ionosonde (grey) calculated BTEC/ITEC.

As seen in Figure 8a, the electron density in the *F* region had significant increase during 14 December compared with 13 December. As expected, the TEC along with N_mF_2 increased significantly during the daytime of 14 December (Figures 8b and 8d), and h_mF_2 (Figure 8c) increased by 60 km associated with the PPEF [*Lei et al.*, 2008]. During the main phase on 15 December, N_mF_2 and TEC showed an obvious negative phase when h_mF_2 declined to about 160–170 km. Namely, the G condition also occurred on 15 December. Interestingly, Figure 8d shows that the ISR and ionosonde derived BTEC/ITEC were constant on 3 days. This indicates that the topside and bottomside electron density profiles changed similarly for both positive and negative ionosphere phases, and it was generally higher than BTEC/GPS-TEC at night since the ratio BTEC/GPS-TEC underwent stronger diurnal variation and became smaller at night. Additionally, the BTEC/GPS-TEC on 15 December was a little smaller than that on other 2 days. Since the ISR derived BTEC/ITEC did not change, the smaller BTEC/GPS-TEC on 15 December should be associated with the contribution of the plasmasphere to the full TEC.

5. Discussion

We utilized ground-based GPS receivers, ionosondes, and ISRs to study the contribution of TEC above and below the F_2 peak to total TEC in ionosphere during the September 2005 and December 2006 storms at low and middle latitudes. It was found that the BTEC/ITEC from both ionosonde and ISR data varied little, whereas BTEC/GPS-TEC experienced significant diurnal variations during both quiet and storm times. Besides the contribution of PTEC to GPS TEC, *Belehaki and Tsagouri* [2002] attributed the differences between the ionosonde BTEC/ITEC and BTEC/GPS-TEC to the uncertainty of the GPS TEC retrieval at nighttime. If this is the case, the uncertainty of satellite and receiver bias could not cause so consistent pattern in the differences between BTEC/ITEC and BTEC/GPS-TEC. Smaller BTEC/GPS-TEC at night might be related to a larger contribution of PTEC to GPS TEC. Moreover, BTEC/GPS-TEC during the negative phase exhibited a decline during both storms. This indicates that when electron densities were eaten away during the negative phase, the contribution of PTEC to TEC became larger relatively.

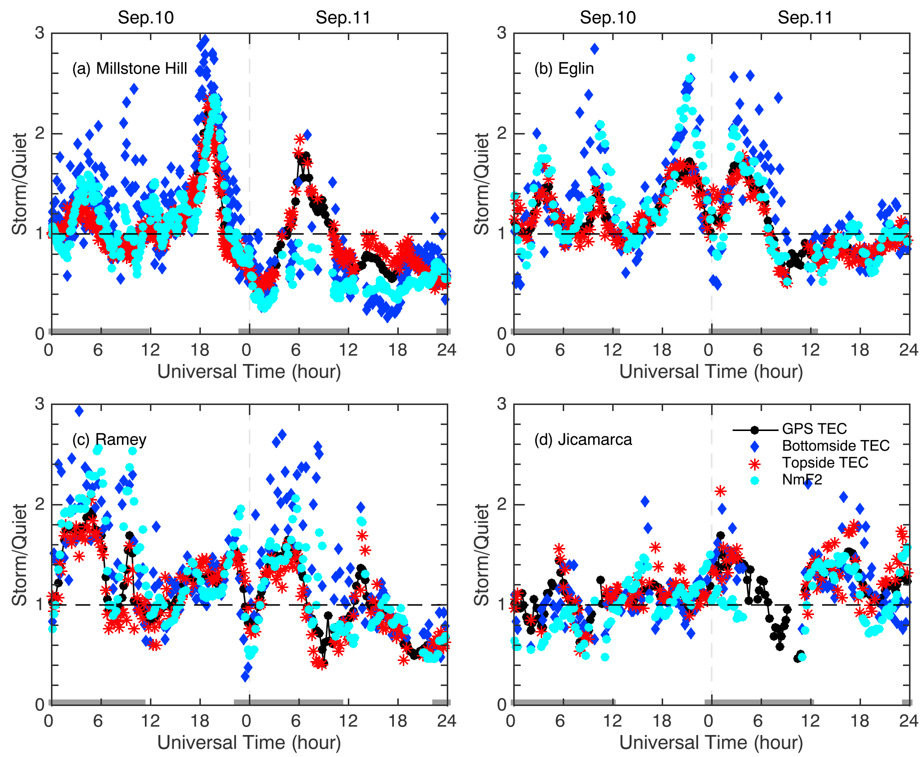

Figure 9. Relative changes of N_mF_2 and bottomside, topside and GPS TECs at Millstone Hill, Eglin, Ramey, and Jicamarca on the storm days 10–11 September 2005 with respect to the quiet time references. The observations on 9 September instead of 8 September were used as the quiet time references due to data gaps in the ionosonde observations on 8 September.

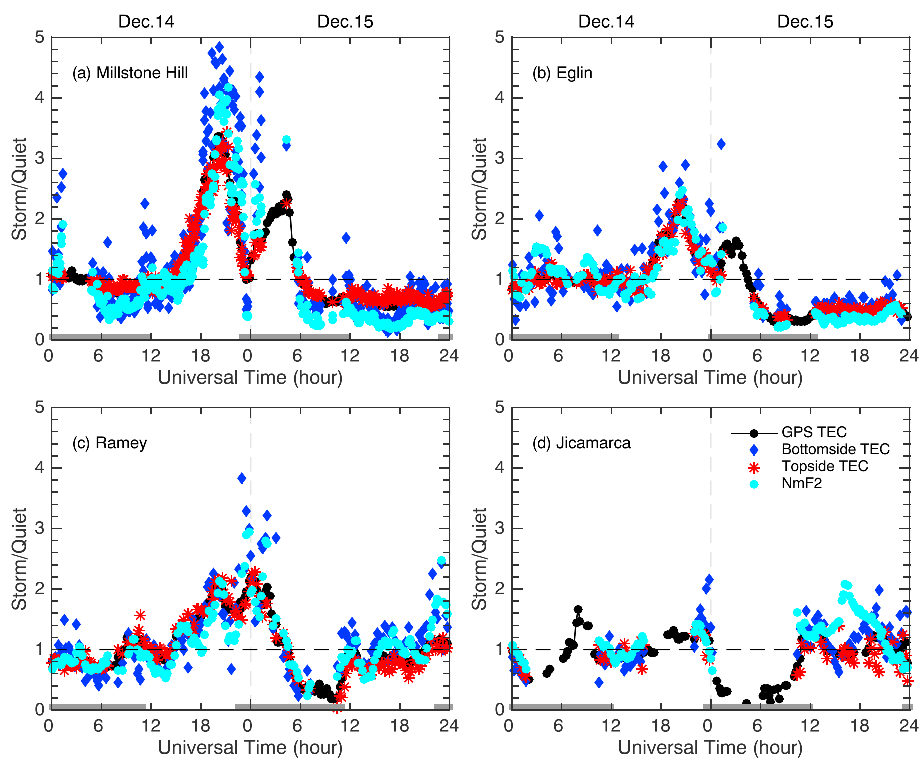

Figure 10. Relative changes of N_mF_2 and bottomside, topside and GPS TECs at Millstone Hill, Eglin, Ramey, and Jicamarca on the storm days 14–15 December 2006 with respect to the quiet time reference on 13 December.

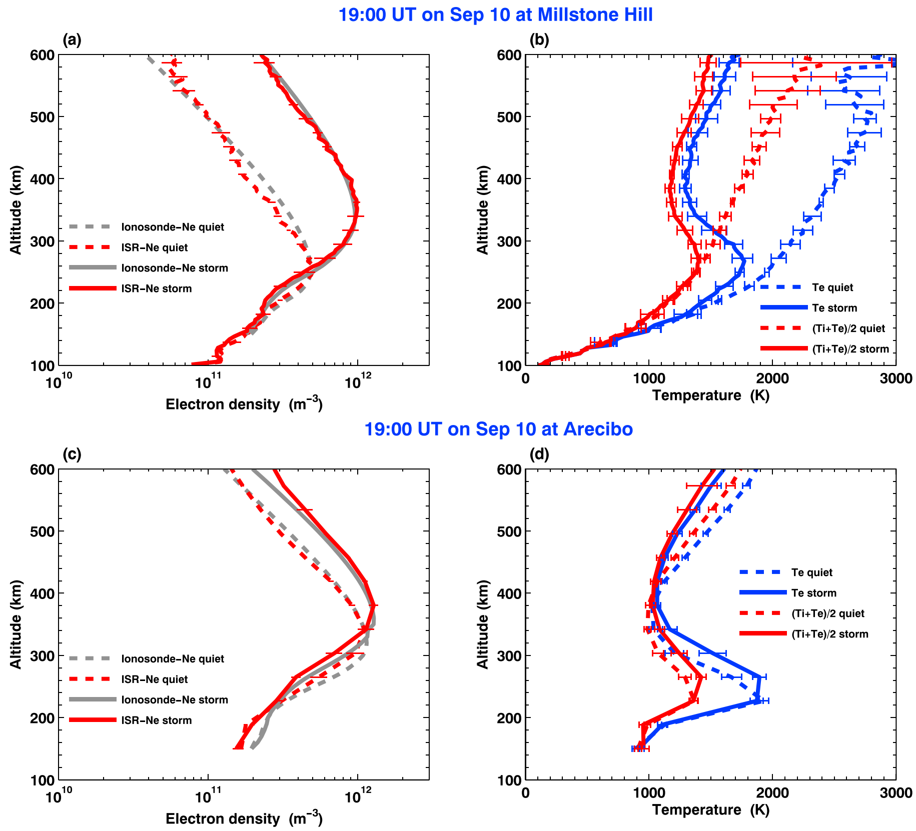

Figure 11. (left) Electron density and (right) plasma temperature profiles over Millstone Hill (top) and Arecibo (bottom) at 19:00 UT on 9–10 September 2005. The dashed lines represent the quiet time references on 9 September and the grey lines in Figures 11a and 11c stand for ionosonde electron density profiles. T_e and T_i represent electron and ion temperatures, respectively.

As shown in Figures 4, 5, and 8, the ionosonde derived BTEC/ITEC was consistent with that from the ISR observations at Millstone Hill and Arecibo during the daytime. It is also interesting that the daytime ISR BTEC/ITEC on the storm days was almost the same as that on the quiet days. According to previous discussion, $\frac{\tau_T}{\tau_B}$ should not change obviously during both storms. That explained why the daytime ionosonde derived ITEC was in agreement with the GPS TEC. *Lei et al.* [2015] reported the topside effective thickness had stronger increase than the bottomside ionosphere did during the 2003 October superstorms when the ionosonde derived ITEC should be much smaller than the GPS TEC at low and middle latitudes. In addition, in the equatorial region (Jicamarca) the daytime BTEC/GPS-TEC was much larger than the corresponding BTEC/ITEC. This indicated that the equatorial topside profile from the ionosonde extrapolation was stretched too much so that the topside scale height was much larger than the bottomside ionosphere.

As discussed previously, the ratios BTEC/ITEC and BTEC/GPS-TEC can be related with $\frac{\tau_T}{\tau_B}$. For instance, if BTEC/ITEC = 0.3, $\frac{\tau_T}{\tau_B}$ would be about 2; for BTEC/ITEC = 0.2, $\frac{\tau_T}{\tau_B}$ is as high as 4. Therefore, it should be common that the absolute changes in the topside TEC are much larger than in the bottomside TEC. As suggested in *Lei et al.* [2015], the relative change of TEC can be written as $\frac{\sigma \text{TEC}}{\text{TEC}} = \frac{\sigma N_m F_2}{N_m F_2} + \frac{\sigma \tau}{\tau}$. Here we also compared relative changes of TECs (bottomside TEC, topside TEC, and GPS TEC) with the relative change of N_mF_2 to examine the similarities and differences in the topside and bottomside response to the geomagnetic storm. Figures 9 and 10 show the relative change of bottomside TEC, topside TEC, and GPS TEC, and N_mF_2 during the September 2005 and December 2006 storms, respectively. Here the topside TEC represents the difference between GPS TEC and ionosonde BTEC.

As seen in Figures 9 and 10, the relative changes in the topside TEC were comparable to or even less than those of bottomside TEC and N_mF_2. Again, weaker changes in the topside TEC during the negative phase for both storms might be related with the plasmaspheric contribution. During the positive phase at Millstone Hill on

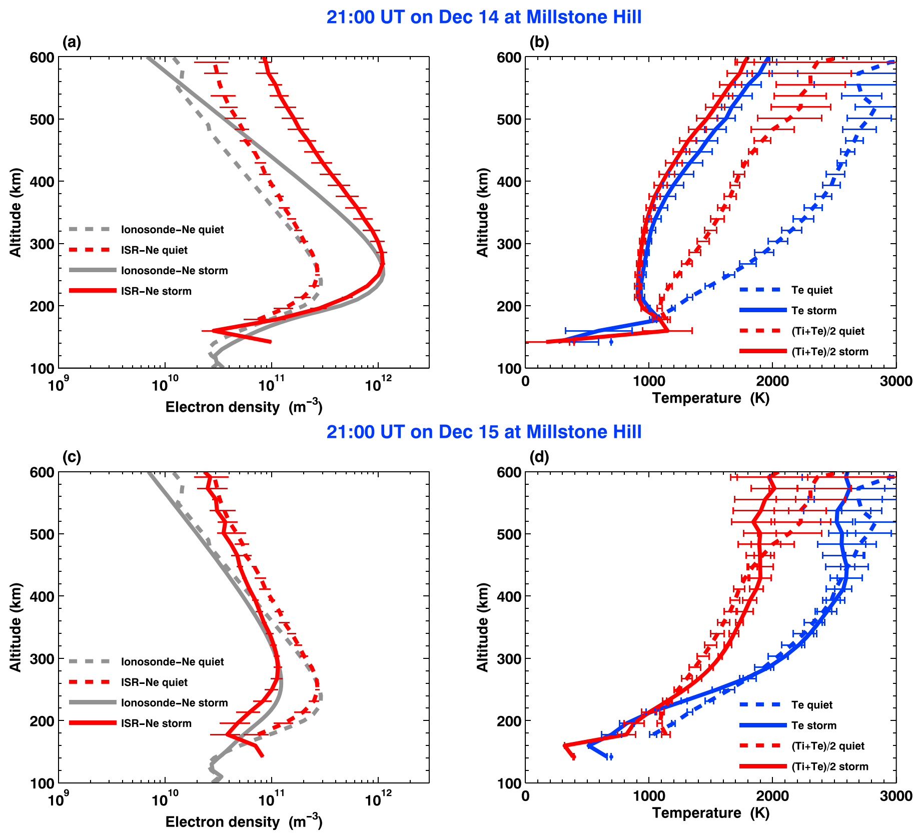

Figure 12. (left) Electron density and (right) plasma temperature profiles at Millstone Hill at 21:00 UT on 13–15 December 2006. The dashed lines represent the quiet time references on 13 December and the grey lines in Figures 12a and 12c stand for ionosonde electron density profiles. T_e and T_i represent electron and ion temperatures, respectively.

10 September and 14 December, and at Eglin on 14 December, the relative changes in the topside TEC were smaller than those of the bottomside TEC. This was consistent with the slight larger BTEC/GPS-TEC in Figures 3 and 7. It indicated that the effective thickness of the topside ionosphere had slight decreases during these periods. Overall, the effective thickness of the topside ionosphere did not change significantly during the daytime of positive phase for both storms.

Figures 11 and 12 show the comparison of the averaged electron density and plasma temperature profiles within 1 h interval during different phases of these two geomagnetic storms. As shown in Figures 11 and 12, the slopes of the topside electron density changes with altitude are similar during quiet and storm times. Again, it suggests that the daytime effective thickness of topside ionosphere did not have significant change during the positive phase for both storms. As shown in Figures 11a and 11c, the ionosonde topside densities were generally consistent with the ISR observations for the September 2005 event. However, for the December 2006 case, at Millstone Hill the ionosonde topside electron densities were significantly lower than the ISR data during both positive and negative ionospheric phases (Figures 12a and 12c). This is also consistent with the results in Figure 8e that the ISR BTEC/ITEC was smaller than ionosonde BTEC/ITEC during the daytime of 13–15 December.

Lu et al. [2008] suggested that the changes of equatorward neutral winds were the primary causes for the observed positive phase in the American sector on 10 September 2005. It is understandable that equatorward neutral winds mainly introduced the changes of electron density locally in the F_2 region so that the topside and bottomside electron densities had similar variations. However, the positive ionospheric phase occurred during the initial phase of the December 2006 storm was resulted from the PPEF effect [*Lei et al.*, 2008]. Supposedly, in addition to the local plasma transport caused by PPEF, fountain effect associated with the PPEF would sweep plasmas in the equatorial region to higher latitudes. Electron density changes at around the EIA crests should be related with the effects of local and horizontal transports. In this sense, the topside ionosphere should gain more predominant enhancement than the bottomside ionosphere would. However, Figures 7 and 10 indicate that the effective thickness of the topside ionosphere at Eglin and Ramey did not have significant change during the daytime of positive phase on 14 December. This is different from the results of *Lei et al.* [2015], who revealed that the relative change of topside TEC was larger than bottomside TEC during the October 2003 superstorms.

In addition, the changes of plasma temperatures during the positive phase should also contribute to the smaller relative change in topside TEC than in N_mF_2 and the bottomside TEC seen at Millstone Hill and Eglin. The electron cooling rate via electron-ion collisions is proportional to the square of electron density [*Schunk and Nagy*, 1978], so the electron temperature will decrease during the positive phase. As shown in Figures 11 and 12, significant decreases of electron temperature were observed during the positive phases of both storms. Plasma temperatures underwent obvious decrease above 200 km during positive phase of both storms as compared with their quiet time references (Figures 11b, 11d, and 12b). This would cause a decrease of plasma scale height, and more electrons should diffuse downward [*Rishbeth*, 1975]. Consequently, the relative changes of the topside TEC were weaker than N_mF_2 and the bottomside TEC during the positive ionospheric phase. However, for the negative phase, as shown in Figure 12d, plasma temperatures had much less changes during the December 2006 storm. Thus, the scale height changes associated with the sole temperature effect would be less obvious during the negative phase as compared with the positive ionospheric phase.

Overall, no substantial differences were observed between the bottomside and topside ionosphere during both storms, which was in contrast with the situation in the October 2003 superstorms. It should be noted that only two strong storms were examined to address the relative contribution of the bottomside and topside TEC to the TEC at low and middle latitudes. Studies showed that the F_2 peak electron densities and TEC had similar climatologic response to the geomagnetic storms [e.g., *Matamba et al.*, 2015]. Further statistical study is required to examine the similarities and differences in the bottomside and topside ionosphere to the strong storms in a quantitative way by using the Global Navigation Satellite System and ionosonde network observations.

6. Summary

In this paper, the ionospheric observations from ground-based GPS receivers, ionosondes, and incoherent scatter radars were used to investigate the relative contribution of the bottomside and topside TEC to the TEC at low and middle latitudes during September 2005 and December 2006 storms. We summarize our main results as follows:

1. The contribution of BTEC to the total GPS-TEC (i.e., BTEC/GPS-TEC) showed obvious diurnal variation during both quiet and storm times, and it was larger during the daytime than at night.
2. The BTEC/GPS-TEC during both storms was comparable to the quiet time values except for the negative storm condition when F_2 peak height was very low.
3. The values of the BTEC/ITEC calculated from the ISR data at Millstone and Arecibo did not show notable changes during storm time as compared with quiet time reference. This suggests that the observed storm effects mainly took place at the F_2 peak region for both the positive and negative storm phases for the two events we are focusing on.
4. The calculated BTEC/ITEC from the ISR data and BTEC/GPS-TEC showed significant discrepancy during the negative phase or at night. This implies that the topside electron density away from h_mF_2 does not have such depletion as the F_2 region where electron densities were eaten away during the negative phase or decayed from the daytime profiles.
5. The relative changes of the topside TEC to the quiet time reference during the September 2005 and December 2006 storms were comparable or even weaker than those of the bottomside TEC and peak density N_mF_2. This is different from the results of the October 2003 superstorms, in which the topside ionospheric thickness increased significantly [*Lei et al.*, 2015]. Plasmaspheric contribution and the changes of plasma temperatures might play an important role in modulating the topside ionospheric response to these two severe storms.

Acknowledgments
The ground-based GPS and ISR data were obtained from the MIT Haystack Observatory Madrigal database (http://madrigal.haystack.mit.edu/), and the ionosonde data were downloaded from the DIDBase (http://umlcar.uml.edu/). This work was supported by the National Natural Science Foundation of China (41325017, 41274157, 41274158, and 41421063), the Project of Chinese Academy of Sciences (KZZD-EW-01), the National Key Basic Research Program of China (2012CB825605), the fundamental research funds for the central universities (WK2080000077), and Thousand Young Talents Program of China.

References

Astafyeva, E. I. (2009), Dayside ionospheric uplift during strong geomagnetic storms as detected by the CHAMP, SAC-C, TOPEX and Jason-1 satellites, *Adv. Space Res.*, *43*, 1749–1756.

Astafyeva, E. I., I. Zakharenkova, and E. Doornbos (2015), Opposite hemispheric asymmetries during the ionospheric storm of 29–31 August 2004, *J. Geophys. Res. Space Physics*, *120*, 697–714, doi:10.1002/2014JA020710.

Belehaki, A., and I. Tsagouri (2002), Investigation of the relative bottomside/topside contribution to the total electron content estimates, *Ann. Geophys.*, *45*, 73–86.

Buonsanto, M. J. (1999), Ionospheric storms—A review, *Space Sci. Rev.*, *88*, 563–601.

Gonzalez, W. D., J. A. Joselyn, Y. Kamide, H. W. Kroehl, G. Rostoker, B. T. Tsurutani, and V. M. Vasyliunas (1994), What is a geomagnetic storm?, *J. Geophys. Res.*, *99*, 5771.

Gulyaeva, T., and I. Stanislawska (2013), Deformation of the ionosphere structure during the space wheather events on October–November 2003, *Adv. Space Res.*, *51*, 683–690.

Huang, X., and B. W. Reinisch (2001), Vertical electron content from ionograms in real time, *Radio Sci.*, *36*(2), 335–342, doi:10.1029/1999RS002409.

Lei, J., W. Wang, A. G. Burns, S. C. Solomon, A. D. Richmond, M. Wiltberger, L. P. Goncharenko, A. Coster, and B. W. Reinisch (2008), Observations and simulations of the ionospheric and thermospheric response to the December 2006 geomagnetic storm: Initial phase, *J. Geophys. Res.*, *113*, A01314, doi:10.1029/2007JA012807.

Lei, J., W. Wang, A. G. Burns, X. Yue, X. Dou, X. Luan, S. C. Solomon, and Y. C.-M. Liu (2014), New aspects of the ionospheric response to the October 2003 superstorms from multiple-satellite observations, *J. Geophys. Res. Space Physics*, *119*, 2298–2317, doi:10.1002/2013JA019575.

Lei, J., Q. Zhu, W. Wang, A. G. Burns, B. Zhao, X. Luan, J. Zhong, and X. Dou (2015), Response of the topside and bottomside ionosphere at low and middle latitudes to the October 2003 superstorms, *J. Geophys. Res. Space Physics*, *120*, 6974–6986, doi:10.1002/2015JA021310.

Lu, G., L. P. Goncharenko, A. D. Richmond, R. G. Roble, and N. Aponte (2008), A dayside ionospheric positive storm phase driven by neutral winds, *J. Geophys. Res.*, *113*, A08304, doi:10.1029/2007JA012895.

Mannucci, A. J., B. D. Wilson, D. N. Yuan, C. H. Ho, U. J. Lindqwister, and T. F. Runge (1998), A global mapping technique for GPS-derived ionospheric total electron content measurements, *Radio Sci.*, *33*(3), 565–582, doi:10.1029/97RS02707.

Mannucci, A. J., B. T. Tsurutani, B. A. Iijima, A. Komjathy, A. Saito, W. D. Gonzalez, F. L. Guarnieri, J. U. Kozyra, and R. Skoug (2005), Dayside global ionospheric response to the major interplanetary events of October 29–30, 2003 "Halloween Storms", *Geophys. Res. Lett.*, *32*, L12S02, doi:10.1029/2004GL021467.

Matamba, T. M., J. B. Habarulema, and L.-A. McKinnell (2015), Statistical analysis of the ionospheric response during geomagnetic storm conditions over South Africa using ionosonde and GPS data, *Space Weather*, *13*, 536–547, doi:10.1002/2015SW001218.

Mendillo, M. (2006), Storms in the ionosphere: Patterns and processes for total electron content, *Rev. Geophys.*, *44*, RG4001, doi:10.1029/2005RG000193.

Prölss, G. W. (1995), Ionospheric *F*-region storms, in *Handbook of Atmospheric Electrodynamics*, edited by H. Volland, pp. 195–248, CRC Press, Boca Raton, Fla.

Reinisch, B. W., P. Nsumei, X. Huang, and D. Bilitza (2007), Modeling the F2 topside and plasmasphere for IRI using IMAGE/RPI and ISIS data, *Adv. Space Res.*, *39*, 731–738.

Rideout, W., and A. Coster (2006), Automated GPS processing for global total electron content data, *GPS Solutions*, *10*, 219–228, doi:10.1007/S10291-006-0029-5.

Rishbeth, H. (1975), On the theory of diffusion in the ionosphere, *Geophys. J. R. Astron. Soc.*, *41*, 311–317.

Schunk, R. W., and A. F. Nagy (1978), Electron temperatures in the *F* region ionosphere: Theory and observations, *Rev. Geophys.*, *16*, 355–399, doi:10.1029/RG016i003p00355.

Stankov, S. M., N. Jakowski, S. Heise, P. Muhtarov, I. Kutiev, and R. Warnant (2003), A new method for reconstruction of the vertical electron density distribution in the upper ionosphere and plasmasphere, *J. Geophys. Res.*, *108*(A5), 1164, doi:10.1029/2002JA009570.

Verhulst, T., and S. M. Stankov (2015), Ionospheric specification with analytical profilers: Evidences of non-Chapman electron density distribution in the upper ionosphere, *Adv. Space Res.*, *55*(8), 2058–2069.

Zhao, B., W. Wan, J. Lei, Y. Wei, Y. Sahai, and B. Reinisch (2012), Positive ionospheric storm effects at Latin America longitude during the superstorm of 20–22 November 2003: Revisit, *Ann. Geophys.*, *30*, 831–840.